第 33 卷第 12 期
2017 年 12 月

无 机 化 学 学 报
CHINESE JOURNAL OF INORGANIC CHEMISTRY

Vol.33 No.12
2311-2321

AAO 辅助三唑亚铁纳米材料：一维限制生长和二维表面成膜及自旋转换性能

李志华[1] 王玉侠[1] 邱 丹[1] 李在均[1] 顾志国*,[1,2]

([1]江南大学化学与材料工程学院,无锡 214122)

([2]合成胶体与生物技术教育部重点实验室,无锡 214122)

摘要：通过连续多步自组装的方式分别将三唑亚铁(SCO1)和氨基三唑亚铁(SCO2)自旋转换纳米材料生长于氧化铝模板(AAO)的孔道内和表面上。利用扫描电镜(SEM)、红外光谱(IR)、粉末 X 射线衍射(PXRD)、拉曼光谱(Raman)等手段对 SCO1-1D+2D 和 SCO2-1D+2D 纳米材料进行表征,SEM 表明随着自组装时间的增加,球状的 SCO 纳米颗粒生长于 AAO 孔道内,并逐渐形成 1D 的纳米结构,而在 AAO 表面则形成致密均匀的 SCO-2D 薄膜。两种 SCO-1D+2D 纳米粒子都具有两步自旋行为(SCO1-1D+2D:$T_{c1}\uparrow$=319 K,$T_{c1}\downarrow$=313 K,$T_{c2}\uparrow$=381 K,$T_{c2}\downarrow$=340 K;SCO2-1D+2D:$T_{c1}\uparrow$=181 K,$T_{c1}\downarrow$=155 K,$T_{c2}\uparrow$=246 K,$T_{c2}\downarrow$=233 K)。对相应的 SCO-1D 和 SCO-2D 磁性结果表明,两步自旋转换行为的产生是由于 SCO 组装体形貌的差异。其中,低温区的自旋转换行为是由生长于 AAO 表面的 SCO-2D 自旋转换性能所致，而发生在更高温度的第二阶段的自旋转换行为则归因于生长于 AAO 孔道内的 SCO-1D 的自旋转换性能。

关键词：纳米材料；氧化铝模板；自组装；两步自旋转换

中图分类号：TB33 **文献标识码**：A **文章编号**：1001-4861(2017)12-2311-11

DOI:10.11862/CJIC.2017.200

AAO Assisted 1D Confined Assembly and 2D Surface Filming of Iron(Ⅱ) Triazole Nanomaterial and Spin-Crossover Properties

LI Zhi-Hua[1] WANG Yu-Xia[1] QIU Dan[1] LI Zai-Jun[1] GU Zhi-Guo*,[1,2]

([1]*School of Chemistry and Material Engineering, Jiangnan University, Wuxi, Jiangsu* 214122, *China*)

([2]*Key Laboratory of Synthetic and Biological Colloids, Ministry of Education, Wuxi, Jiangsu* 214122, *China*)

Abstract: Iron(Ⅱ) triazole (SCO1) and iron(Ⅱ) 4-amino-triazole (SCO2) spin-crossover (SCO) nanomaterials were assembled in the channel and on the surface of anodic aluminum oxide (AAO) templates simultaneously by a facile sequential multistep assembly method. The obtained SCO1-1D+2D and SCO2-1D+2D nanomaterials have been characterized by SEM, FT-IR, PXRD, and Raman spectra. SEM images show that spherical SCO NPs growing in the channel of AAO templates aggregate with time going on, and assemble as 1D nanostructure. While those growing on the surface of AAO substrates assemble as uniform and dense 2D SCO film. It is interesting that both SCO-1D+2D nanostructures present a special two-step spin-crossover behaviour with hysteresis loops (SCO1-1D+2D: $T_{c1}\uparrow$=319 K, $T_{c1}\downarrow$=313 K, $T_{c2}\uparrow$=381 K, $T_{c2}\downarrow$=340 K; SCO2-1D+2D: $T_{c1}\uparrow$=181 K, $T_{c1}\downarrow$=155 K, $T_{c2}\uparrow$=246 K, $T_{c2}\downarrow$=233 K). The magnetic measuring of SCO-1D and SCO-2D indicates that the two-step SCO behaviour results from the different assembly morphologies of SCO. The first step spin transition at lower temperature is ascribed to the properties of 2D SCO films growing on the surface of AAO templates, while the

收稿日期:2017-05-28。收修改稿日期:2017-07-16。

国家自然科学基金(No.21771089)和中央高校基本科研业务经费(No.JUSRP51725B,JUSRP51513)资助。

*通信联系人。E-mail:zhiguogu@jiangnan.edu.cn

transition in the second step at higher temperature can be attributed to the 1D SCO confined assembly growing in the channel of AAO membranes.

Keywords: nanomaterials; anodic aluminum oxide (AAO) templates; self-assembly; two-step spin-crossover behavior

0 Introduction

Spin-crossover (SCO) compounds are well known as a class of bistable materials, displaying a reversible switching between low spin (LS) state and high spin (HS) state of d^4~d^7 transition metal centres in response to the external perturbations such as pressure, temperature, illumination or magnetic fields[1]. Recently, SCO nanomaterials have drawn the widespread attention as their spin conversion can be modified by size, morphologies and preparation method[2], which offers various possible applications in molecular switches, memory devices, sensors and displayers[3]. However, assembling SCO nanoparticles (NPs) still shows more challenges while affords new and exciting opportunities for the development of SCO devices. Among the configurations of SCO nanoparticle assembly, one-dimensional (1D) confined assembly and two-dimensional (2D) multi-layered films may be considered as useful models to explore the effect of dimensionality on SCO property[4]. Reliable thin-film etching[5], template-assisted electrodeposition routes[6] and template-assisted assembly methods[7] have been established to obtain the 1D SCO nanomaterials. Meanwhile, several methods have been used to fabricate SCO nanomaterials as two-dimensional (2D) films, including Langmuir-Blodgett (LB) deposition[8], surface-assisted molecular self-assembly[9], spin coating[10], dip/drop casting[11], constructive methods[12] and vacuum sublimation[13]. The research for SCO 1D and 2D nano-entities suggests that the assembly morphologies have a strong influence on spin conversion property. To the best of our knowledge, there is no report on the formation of the nanostructure combining the 1D confined assembly and 2D film of SCO compounds. While fabricating the nanostructures consisted of 1D and 2D assembly morphologies simultaneously probably can impart the SCO nanomaterials special spin-crossover properties, which provide a platform for the application of SCO materials into functional devices. With this perspective, we envisaged to prepare one SCO compound with different dimensional assembly morphologies by a facile template assisted self-assembly method.

In order to fabricate the nanomaterial consisted of 1D confined assembly and 2D film simultaneously, it′s crucial to select the suitable template. Anodic aluminium oxide (AAO) membrane is considered as an ideal candidate since: (1) AAO membranes form a cylindrically close packed ordered structure, which can give access to SCO compound growing into their channels as 1D SCO confined assembly[14]. (2) The abundant -OH on the surface of AAO membranes can coordinate with metallic centres[15], which makes 2D SCO film growing on AAO surface possible. The typical iron(Ⅱ)-triazole polymers, $[Fe(Htrz)_2(trz)](ClO_4)$[16] (SCO1) and $Fe(NH_2trz)_3](ClO_4)_2$[17] (SCO2) (Htrz=1,2,4-triazole, NH_2trz =4-amino-1, 2, 4-triazole) undergoing spin transition with well-defined thermal hysteresis loops close to room temperature are selected as model compounds in this paper to study their assembly in the channel and on the surface of AAO templates. Detailed scanning electron microscopy (SEM) will be presented to characterize the formation of the novel nanostructures. And the effect of different dimensional assembly morphologies on their magnetic properties will also be discussed.

1 Experimental

1.1 Chemical materials

$Fe(ClO_4)_2\cdot 6H_2O$, Htrz (Htrz=1,2,4-triazole), NH_2trz (4-amino-1,2,4-triazole), and ethanol were all reagent grade and purchased from Sigma-Aldrich, and could be used without further purification. Ultrapure milli-Q water (18.2 MΩ·cm) was used in all experiments. AAO (≥99%) were purchased from LeSen nano science and technology co., LTD, and without any purification.

1.2 Physical measurements

Fourier transform infrared (FT-IR) spectra were recorded by FALA2000 FT-IR spectrometer (ABB Bomen Canada) (KBr disk). Powder X-ray diffraction (PXRD) patterns were collected on a D8 Advance X-ray diffractometer (Bruker AXS Germany) with Cu $K\alpha$ radiation (λ=0.154 046 nm) in a 2θ range from 5° to 60° at the speed of 2°· min^{-1} at room temperature. The operating voltage and current are 40 kV and 40 mA, respectively. Raman spectra of these nanomaterials were obtained from Invia Raman spectra (Reinshaw England) with 785 nm excitation line. The laser power intensity was adjusted by changing the percentage of 280 mW, the largest laser power intensity in 785 nm excitation line. SEM images were operated by S4800 scanning electron microscope (SEM) (Rili Japan) at an operating voltage of 2 kV. Magnetic measurements were carried out by a MPMS-XL-7 super strong quantum interference magnetometer (Quantum Design US). The direction of the magnetic field is parallel to the sample. The samples were testing at two temperature stages with a heating and cooling sweep rate of 3 K·min^{-1}. The SCO phenomenon of each samples were clearly displayed by HS fraction vs T curves, in which HS fraction refers to the ratio of iron(Ⅱ) at high spin state. Data were corrected for the diamagnetic contribution calculated from Pascal constants.

1.3 Synthetic procedures

1.3.1 Synthesis of SCO1-1D+2D and SCO2-1D+2D nanomaterials

AAO (Φ=300~400 nm) templates were immersed into 1 mol·L^{-1} ethanol solution of $Fe(ClO_4)_2 \cdot 6H_2O$ for 1 h. Then, these AAO templates were washed with ethanol carefully to remove the redundant Fe^{2+}. Afterwards, the templates were soaked into 3 mol·L^{-1} ethanol solution of Htrz for 1 h, and then also washed with ethanol carefully to make sure that the growth rate of 1D SCO nanostructure is much faster than that of the 2D SCO nanoassemblies. Repeat the procedure above for 1, 6, 12, 24 times respectively to obtain a series of SCO1-1D +2D nanoassembly with cycle number of 1, 6, 12, 24 times. SCO1-1D +2D spin-crossover nanomaterials were obtained by washing with 4 mL ethanol for three times and dried in vacuum at 45 ℃ overnight. Fabrication of SCO2-1D+2D was similar to that of the SCO1-1D +2D except replacing the Htrz with NH_2trz.

1.3.2 Synthesis of SCO1-2D and SCO2-2D nanomaterials

Firstly, AAO (Φ=30~40 nm) templates were soaked into 1 mol·L^{-1} ethanol solution of $Fe(ClO_4)_2 \cdot 6H_2O$ for 5 min, and put into ethanol for 1 min, successively. Then they were moved into 3 mol·L^{-1} ethanol solution of Htrz for 5 min, followed by putting into ethanol for 1 min. After recycling for 24 times, they were washed by ethanol for three times to remove the superfluous nanoparticles and dried at 45 ℃ in vacuum for 12 h. The synthesis of SCO2-2D was similar to that of SCO1-2D, but NH_2trz was used instead of Htrz.

1.3.3 Synthesis of SCO1-1D and SCO2-1D nanomaterials

AAO (Φ=300~400 nm) was put into 1 mol·L^{-1} ethanol solution of $Fe(ClO_4)_2 \cdot 6H_2O$ for 1 h, followed by washing with ethanol carefully for three times to remove Fe^{2+} on the surface of AAO templates. Then these templates were transferred to 3 mol·L^{-1} ethanol solution of Htrz for 1 h and washed with ethanol carefully for three times, successively. After repeating the above procedure for 24 times, SCO1-1D nanomaterials were prepared by washing with ethanol three times and drying at 45 ℃ in vacuum for 12 h. The fabrication of SCO2-1D was similar to that of SCO1-1D using NH_2trz instead of Htrz.

2 Results and discussion

The AAO template-assisted SCO nanostructures are prepared via a facile sequential multistep assembly method (Fig.1)[18]. Firstly, AAO templates were soaked into the ethanol solution of $Fe(ClO_4)_2 \cdot 6H_2O$ at room temperature. This procedure can make sure that the Fe^{2+} coordinated with -OH in the channel of the AAO templates adequately by capillarity, and -OH on the surface of AAO templates by surface deposition. Then, these AAO templates were immersed into the ethanol solution of Htrz or NH_2trz to coordinate with Fe^{2+} attached to the AAO templates.

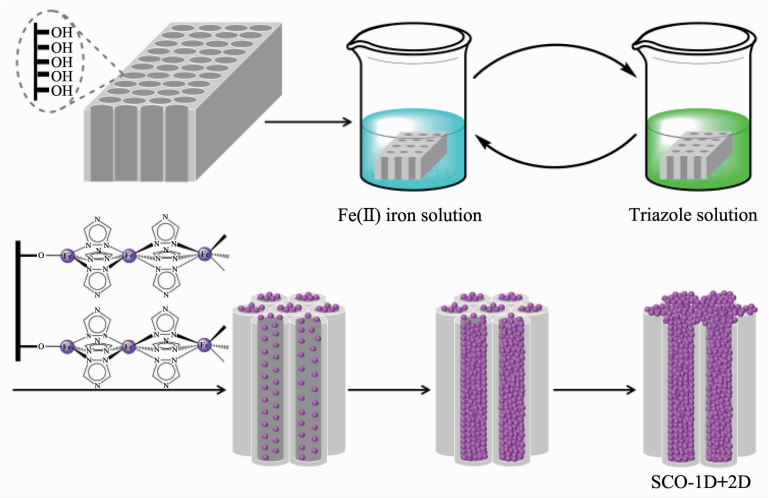

Fig.1 Scheme of the synthesis for SCO nanocomposite with sequential multistep assembly method

Repeating the procedure above to insure the SCO NPs gradually deposited on the surface and filled in the channel of AAO templates. The sequential multistep assembly approach introduced here shows the merit that the growth and nucleation of the 1D and 2D SCO nanostructures based on the AAO templates can be tuned by adjusting the assembly cycle numbers.

IR spectra of SCO1-1D+2D and SCO2-1D+2D nanomaterials indicate that the bands observed for two nanostructures are mainly due to vibrations of the triazole derivative ligand, slightly perturbed by coordination (Fig.S1). In particular, the vibrational modes at *ca.* 1 221, 1 496 and 1 453 cm^{-1} can be attributed to the ring stretching of the triazole ligands. The peak at *ca.* 634 cm^{-1} is referred to the out-of-plane vibration of the triazole ligand [19]. Furthermore, the ClO_4^- anion possesses characteristic vibrational frequencies at *ca.* 941 and 1 120 cm^{-1} [20]. The peaks of near 3 360 and 3 284 cm^{-1} refer to the stretching of $-NH_2$ on triazole ligands. IR result implies the formation of AAO-assisted SCO materials preliminarily.

The powder X-ray diffraction (PXRD) patterns of the as-prepared SCO1-1D+2D and SCO2-1D+2D nanomaterials are shown in Fig.S2. The diffraction peaks (2θ) of the SCO1-1D+2D nano-assemblies at *ca.* 10°, 18°, 25° are consistent with the standard XRD data for the bulk $[Fe(Htrz)_2(trz)](ClO_4)$[19,21]. While the diffraction peaks for SCO2-1D+2D nanomaterials correspond to the crystalline $[Fe(NH_2trz)_3](ClO_4)_2$ reported previously[21]. PXRD analysis indicates the existence of $[Fe(Htrz)_2(trz)](ClO_4)$ and $[Fe(NH_2trz)_3](ClO_4)_2$ in the AAO membrane.

To identify the SCO compound assembled in the channel and on the surface of AAO templates, Raman microscopy measurements were carried out at 785 nm. It was obvious that the characteristic Raman signals were preserved in the obtained AAO membranes assisted nanomaterials (Fig.S3). The wavenumber values below 400 cm^{-1} are assigned to the metal-ligand Fe-N vibrations, and those between 900 and 1 600 cm^{-1} are related to the vibrations of triazole ring[17b,21a,23]. Typically, the drastic changes in the low wavenumber region below 400 cm^{-1} are applied to monitor the spin state of the iron(Ⅱ) triazole complexes. In a complete spin conversion, the Raman modes at 106 cm^{-1} display intensely in the HS state and vanish in the LS state, while the Raman signals at 286 cm^{-1} corresponds to the LS state[24]. Raman spectra further demonstrate the SCO compound growing on the AAO substrates.

The obtained SCO-1D+2D nanomaterials by AAO templates with channel size of 300~400 nm were characterized by the scanning electron microscope (SEM) measurement to study their nucleation and growth of SCO NPs on AAO substrates. Fig.2 showed the SEM images of SCO1 NPs on the surface and in the internal channels of AAO templates with different assembly cycle numbers (n=1, 6, 12 and 24). At the beginning (reacting for only 1 cycle), almost no SCO1 NPs are found in the substrates in Fig.2a and 2b.

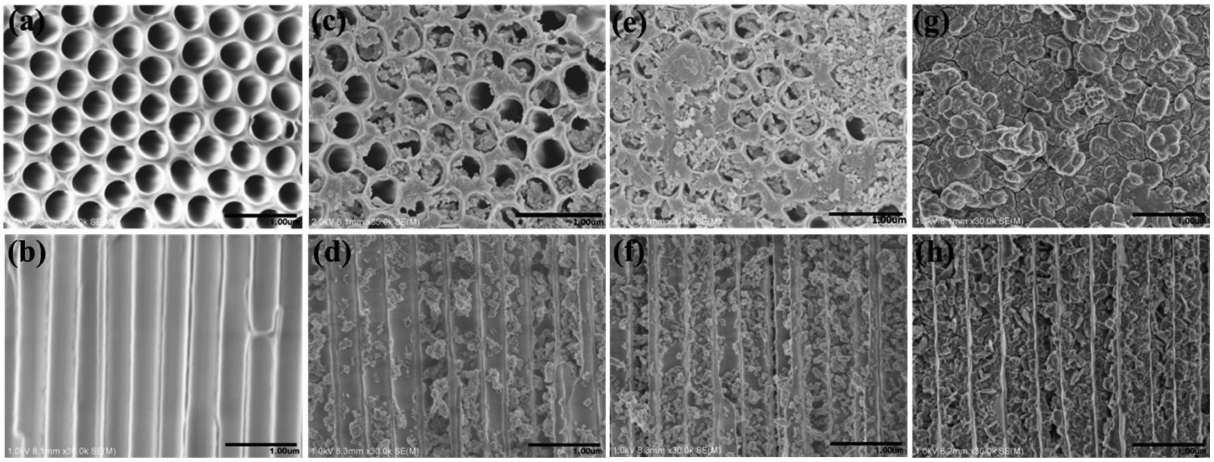

(a) and (b), (c) and (d), (e) and (f), (g) and (h) correspond to 1, 6, 12, 24 cycles, respectively

Fig.2　SEM images of SCO1-1D+2D with different cycles

With reacting for 6 cycles, SCO1 NPs could be clearly observed on the surface and in the cross-section of AAO templates (Fig.2c and 2d), shaped as sphere and most of the NPs look inhomogeneous due to the aggregation. This reveals the beginning of growth and nucleation of the SCO1 crystals. As expected, SCO1 NPs in the channel of AAO templates augmente largely by the number of cycles adding (Fig. 2d and 2f). Besides, the deposition of SCO1 NPs on the surface of AAO membranes grows more slowly than that in the cross-section of AAO templates (Fig. 2c and 2e). This is attributed to the procedure of washing with ethanol carefully. As the cycle number increased, more and more NPs stacked in the channel and on the surface of AAO membrane templates. When 24 cycles have been realized, the surfaces of AAO templates are covered with aggregated SCO1 NPs assembling as uniform and dense SCO1 films (Fig.2g), while the AAO membrane channels are filled with SCO1 NPs accumulated as one-dimensional confined nanostructure (Fig.2h). It should be mentioned that there are two different dimensional assembly morphologies of SCO1 in the SCO1-1D +2D, which intuitively confirms the successful synthesis of the special SCO1-1D+2D nanomaterials. Furthermore, the deposition and assembly morphology of SCO1 NPs on the surface and in the channels of AAO templates are able to be adjusted by controlling the reaction cycle numbers in two precursor solutions.

In order to study the growth and nucleation of different assembly morphologies of SCO compound respectively, the SCO1 assemblies growing on the surface of AAO templates (SCO1-2D) and in the channel of AAO templates (SCO1-1D) were obtained by choosing AAO templates with different channel size. The SCO1-2D nanomaterials are fabricated by AAO templates with narrow channel size of 30~40 nm to ensure the SCO NPs only growing on the surface of AAO membranes. Accordingly, the synthesis of SCO1-1D nanomaterials is realized by the assist of AAO templates with large channel size (300~400 nm), and washing with ethanol carefully to make sure that no SCO1 NPs grow on the surface of AAO membranes. Fig.3a displays that the spherical and inhomogeneous SCO1 NPs grow on the surface of AAO templates assembling as 2D film with large surface areas, while no SCO1 NPs is found on the AAO channels (Fig.3b). In contrast, Fig.3c and 3d suggest that the homogeneously spherical SCO1 NPs accumulate only in the internal channels of AAO membranes, and form the 1D confined SCO1 nanostructures.

To study the influence of iron(Ⅱ)-triazole NPs with different organic ligands by the support of AAO membrane templates, SCO2-1D +2D, SCO2-2D and SCO2-1D nanostructures via the similar methods were synthesized, and SEM images were set out in Fig.4 and Fig.5. In SCO2-1D +2D, there are some little $[Fe(NH_2trz)_3](ClO_4)_2$ NPs growing in the channel of

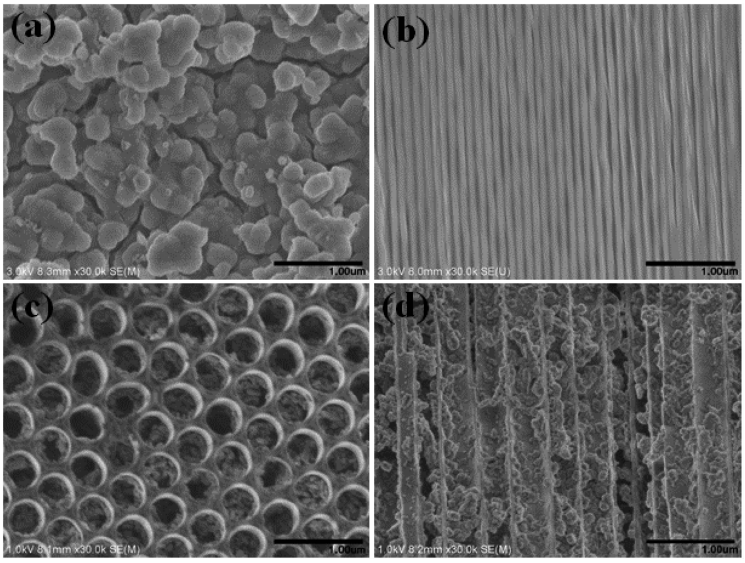

Fig.3 SEM images of SCO1-2D (a, b) and SCO1-1D (c, d)

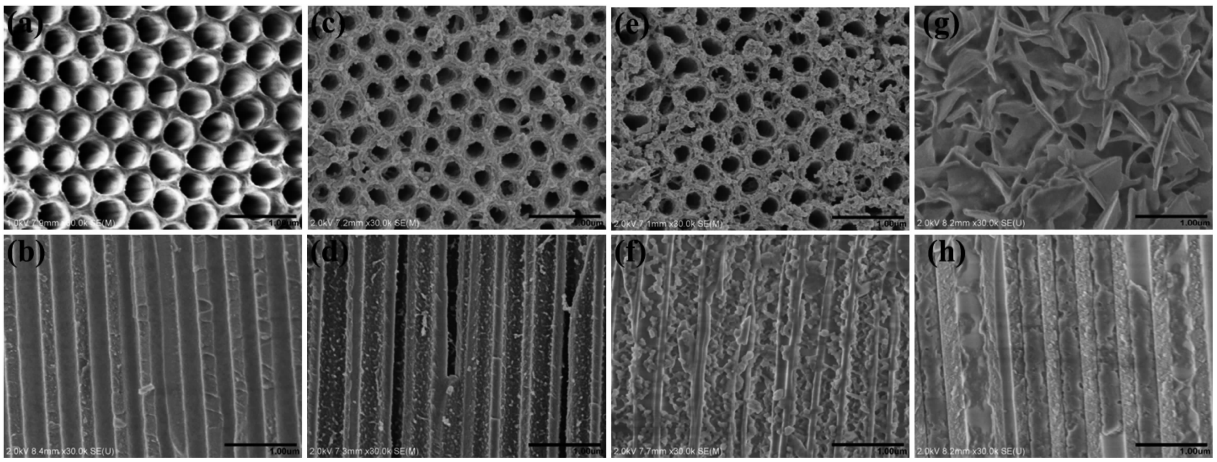

(a) and (b), (c) and (d), (e) and (f), (g) and (h) correspond to 1, 6, 12, 24 cycles, respectively

Fig.4 SEM images of SCO2-1D+2D with different cycles

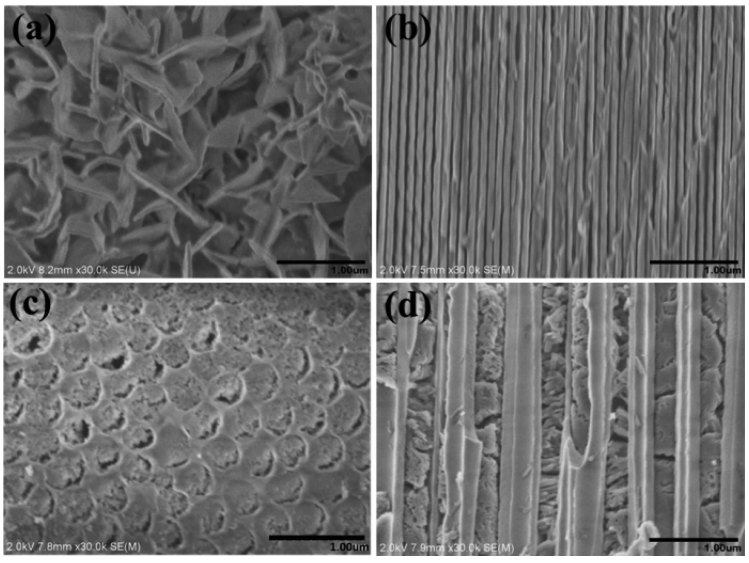

Fig.5 SEM images of SCO2-2D (a, b), SCO2-1D (c, d)

AAO membranes when reacting for the first cycle. As the reacting cycles added, the size and amount of these NPs increase gradually. Some NPs occurred to stack at a certain extent, as shown in Fig.4c~4f. After cycling for 24 times, the SCO2 NPs on the surface of the membranes are lamellate-like and stacked as 2D SCO films, and those accumulated in the channels of templates fill most volume of the apertures, aggregating as 1D confined nano-assembly. The surface of SCO2-2D are arranged of $[Fe(NH_2trz)_3](ClO_4)_2$ laminar film for the intensive surface deposition effect. Similarly, the SCO2 NPs in SCO2-1D accumulate in the channels and there is almost nothing on the surface of the AAO membranes. Comparison in morphological analysis of SCO1-1D+2D and SCO2-1D+2D implies that the organic ligands have an influence on the morphologies of the iron(Ⅱ) triazole nanoassemblies. Furthermore, it also demonstrates that the confined growth and surface filming effect of AAO templates have a directive effect on the formation of different assembly morphologies of $[Fe(Htrz)_2(trz)](ClO_4)$ and $[Fe(NH_2trz)_3](ClO_4)_2$ NPs.

To investigate the spin-crossover property of the obtained AAO-assisted SCO nanomaterials with different dimensional assembly morphologies, the magnetic property of the SCO1-1D+2D were measured over the temperature range from 300 to 400 K with a heating and cooling sweep. As shown in Fig.6a, the spin-crossover behaviour of SCO1-1D+2D shows a two-step spin transition property which is interesting to be observed in one triazole-based iron(Ⅱ) polymer. The first step revealed a gradual and narrow hysteresis loop of *ca.* 6 K with spin transition temperatures $T_{c1}\uparrow$ =319 K in the warming process and $T_{c1}\downarrow$ =313 K in the cooling process. While for the second step, it exhibits a rather steep and broad spin-crossover behaviour, and the transition temperatures in the heating and cooling mode appeared at $T_{c2}\uparrow$ =381 K and $T_{c2}\downarrow$ =340 K with a hysteresis loop width of *ca.* 41 K. Compared with the transition temperature of bulk

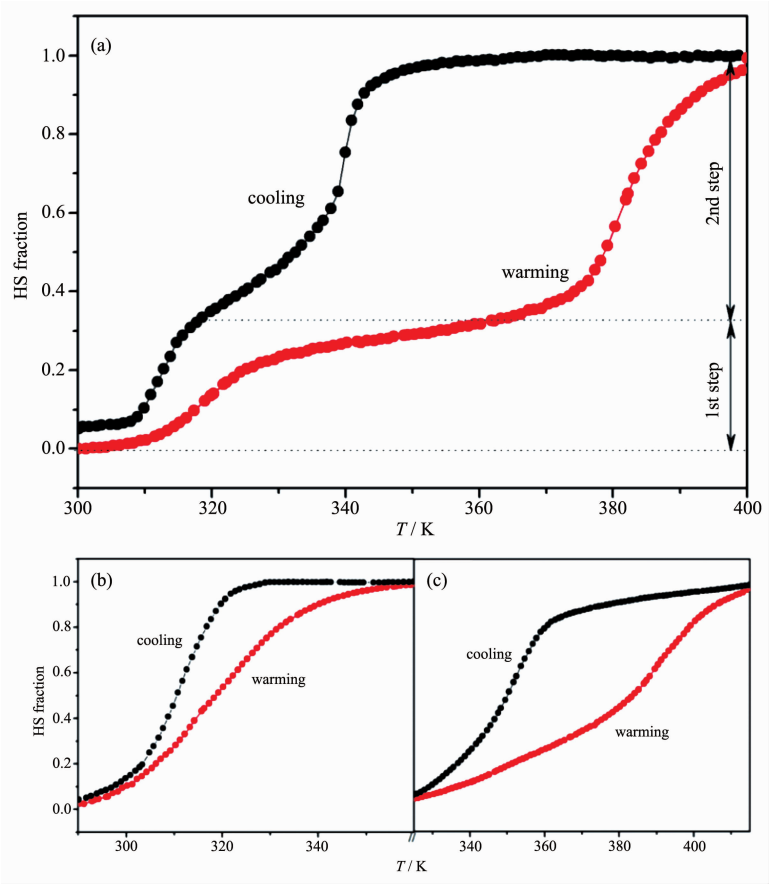

Fig.6　Plots of HS fraction vs *T* for SCO1-1D+2D (a), SCO1-2D (b) and SCO1-1D (c) nanostructures

powder of SCO1 ($T_c\uparrow$ =360 K and $T_c\downarrow$ =339 K, ΔT= 21 K)[16], the first step transition of SCO1-1D+2D moves to a lower temperature with a narrower hysteresis width. While the transition temperatures in the second step shift to a higher region and the hysteresis loop becomes much wider. It can be deduced that this special stepwise spin-crossover behaviour of the SCO1-1D +2D is probably attributed to the different dimensional assembly morphologies of SCO nanomaterials on the surface and in the channels of AAO templates. In order to further study the two-step spin transition behaviour of SCO1-1D +2D nanomaterials, the magnetic properties of SCO1-2D and SCO1-1D were measured (Fig.6b and 6c). The transition temperatures of SCO1-2D are $T_c\uparrow$ =340 K in warming and $T_c\downarrow$ =320 K in cooling with a hysteresis width of ca. 20 K, which are conformed to the first step SCO behaviour of SCO1-1D +2D nanostructures. Correspondingly, the transition temperatures of SCO1-1D at $T_c\uparrow$ =390 K in warming mode and $T_c\downarrow$ =350 K in cooling mode are in accordance with the second step SCO behaviour of SCO1-1D+2D nanostructures. However, contrasting the stepwise SCO behaviour of SCO1-1D +2D with SCO1-2D and SCO1-1D nanomaterials, it can be clearly inferred that the first step transition of SCO1-1D+2D moves to a lower temperature with narrower hysteresis width and the second conversion temperatures of SCO1-1D +2D are also lower than those of SCO1-1D but the wide hysteresis remains almost unchanged. We deduce that this is probably attributed to the influence of the synergistic effect for the combination of two different dimensional assembly morphologies. The nanoparticles growing on the surface of AAO are on 2D templates and grow in a single direction, while the nanoparticles growing on the channel of the AAO are on 1D template and grow in two orientations. Furthermore, contrasting the 1D SCO nano-assembly with 2D SCO nanostructures, the transition temperature of SCO-2D is lower than that of SCO-1D, and there are some reasons to explain : (1)

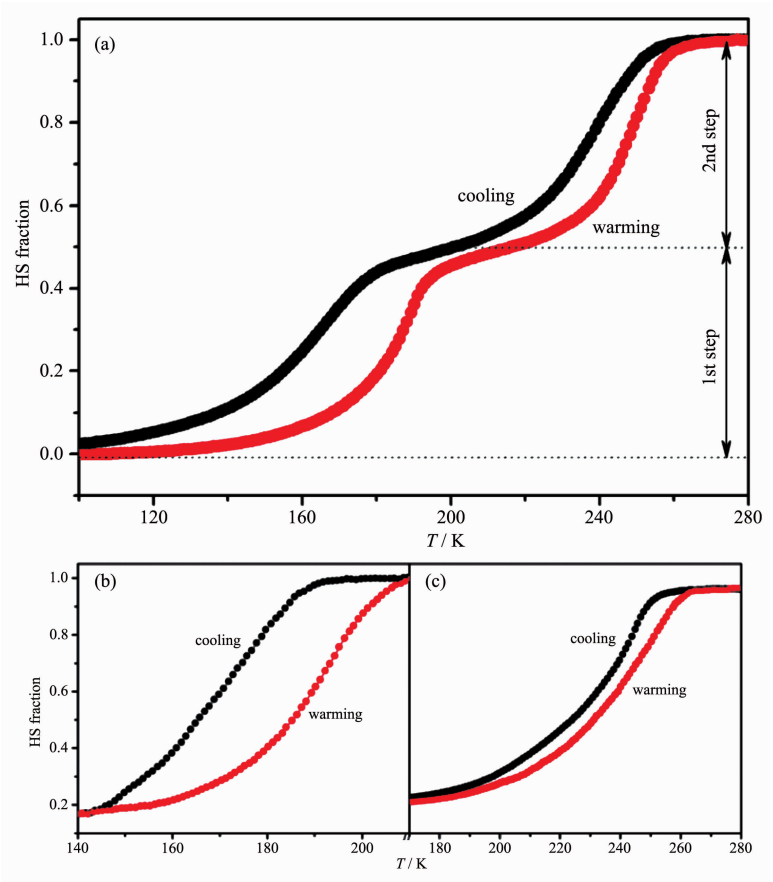

Fig.7 Plots of HS fraction vs T for SCO2-1D+2D (a), SCO2-2D (b) and SCO2-1D (c) nanostructures

The defects for SCO-2D are much more than that of SCO-1D[25,13c]. (2) The difference in growth orientation affects their assembly morphologies, and then indirectly impacts their transition property[26]. In a word, the meaningful SCO1-1D+2D nano-object with two-step SCO property resulting from the morphology effect has been obtained by the support of AAO templates.

Magnetic property of SCO2-1D+2D nanostructures was operated similar to that of the SCO1-1D+2D. As it expected in Fig.7a, the two-step SCO property was also measured in SCO2-1D+2D nanomaterials, but the two transition temperatures were lower than that of the SCO1-1D+2D due to the influence of different organic ligands. The transition temperatures of SCO2-1D+2D are at $T_{c1}\uparrow$ =181 K, $T_{c2}\uparrow$ =246 K in the warming sweep and $T_{c1}\downarrow$ =155 K, $T_{c2}\downarrow$ =233 K in the cooling sweep with the hysteresis loop widths of 26 and 13 K, respectively. Combined with the magnetic analysis of SCO1-1D+2D, it can be inferred that the first step SCO behaviour is attributed to that of the $[Fe(NH_2trz)_3](ClO_4)_2$ film assembling on the surface of the AAO porous templates, and the second step SCO property corresponds to the $[Fe(NH_2trz)_3](ClO_4)_2$ confined nanostructure accumulating in the channel of AAO porous templates. To verify this speculation, the SCO properties of SCO2-2D and SCO2-1D were studied as well, as displayed in Fig.7b and 7c. The transition temperatures of SCO2-2D are $T_c\uparrow$ =190 K in the warming branch and $T_c\downarrow$ =172 K in the cooling branch, while those of SCO2-1D are $T_c\uparrow$ =255 K in the warming mode and $T_c\downarrow$ =243 K in the cooling mode. Contrasting the spin-crossover property of SCO2-1D+2D with SCO2-2D and SCO2-1D nanomaterials, the transition temperatures of SCO2-1D+2D move to a lower region. The results for magnetic analysis of the SCO2-1D+2D, SCO2-2D and SCO2-1D nanomaterials further demonstrate that different assembly morphologies lead to the special stepwise SCO behaviour. What′s more, this also indicates that the change of organic ligands doesn′t have an effect on the appearance of two-step SCO behaviour.

3 Conclusions

In conclusion, a facile and efficient sequential multistep assembly method was employed to synthesize iron (Ⅱ) triazole SCO nanostructures with different assembly morphologies, which exhibit two-step spin-crossover property. There is no report on this spin-crossover phenomenon. The two-step spin transition of SCO-1D+2D corresponds to the SCO NPs assembling on the surface and in the channels of AAO membranes, suggesting that the difference in dimensional assembly morphologies and arrangements of the SCO NPs has a great effect on its SCO property. The fabrication of AAO-assisted 1D+2D spin-crossover nanomaterials provides a novel perspective for producing SCO nanostructure and the basis for the potential application in memory components, data storage and optoelectronic devices.

Supporting information is available at http://www.wjhxxb.cn

References:

[1] (a)Brooker S. *Chem. Soc. Rev.*, **2015**,**44**:2880-2892
(b)Quintero C M, Félix G, Suleimanov I, et al. *Beilstein J. Nanotechnol.*, **2014**,**5**:2230-2239
(c)Bousseksou A, Molnár G, Salmon L, et al. *Chem. Soc. Rev.*, **2011**,**40**:3313-3335
(d)Gütlich P, Gaspar A B, Garcia Y. *Beilstein J. Org. Chem.*, **2013**,**9**:342-391
(e)Gütlich P, Goodwin H A. *Top. Curr. Chem.*, **2004**,**233**:1-47

[2] (a)Mikolasek M, Félix G, Nicolazzi W, et al. *New J. Chem.*, **2014**,**38**:1834-1839
(b)Nagy V, Suleimanov I, Molnár G, et al. *J. Mater. Chem. C*, **2015**,**3**:7897-7905
(c)Giménez-Marqués M, de Larrea M L G S, Coronado E. *J. Mater. Chem. C*, **2015**,**3**:7946-7953
(d)Bartual-Murgui C, Natividad E, Roubeau O. *J. Mater. Chem. C*, **2015**,**3**:7916-7924
(e)Lapresta-Fernández A, Cuéllar M P, Herrera J M, et al. *J. Mater. Chem. C*, **2014**,**2**:7292-7303
(f)WANG Yu-Xia(王玉侠), QIU Dan(邱丹), XI Sai-Fei(奚赛飞), et al. *Chinese J. Inorg. Chem.*(无机化学学报), **2016**, **32**(11):1965-1972b

[3] (a)Linares J, Codjovi E, Garcia Y. *Sensors*, **2012**,**12**:4479-4492
(b)Kahn O, Martinez C J. *Science*, **1998**,**279**:44-48
(c)Rotaru A, Dugay J, Tan R P, et al. *Adv. Mater.*, **2013**,**25**:

1745-1749
(d)Hayami S, Holmes S M, Halcrow M A. *J. Mater. Chem. C*, **2015**,**3**:7775-7778
(e)Bartual-Murgui C, Akou A, Thibault C, et al. *J. Mater. Chem. C*, **2015**,**3**:1277-1285
(f)Molnár G, Salmon L, Nicolazzi W, et al. *J. Mater. Chem. C*, **2014**,**2**:1360-1366

[4] (a)Martinho P N, Rajnak C, Ruben M. *Spin-Crossover Mater.*, **2013**:375-404
(b)Cavallini M. *Phys. Chem. Chem. Phys.*, **2012**,**14**:11867-11876

[5] (a)Thomas L, Hayashi M, Jiang X, et al. *Science*, **2007**,**315**:1553-1556
(b)Woltersdorf G, Back C H. *Phys. Rev. Lett.*, **2007**,**99**:227207

[6] (a)Ebels U, Radulescu A, Henry Y, et al. *Phys. Rev. Lett.*, **2000**,**84**:983-986
(b)Guo L M, Wang X H, Zhong C F, et al. *J. Appl. Phys.*, **2012**,**111**:026104
(c)Reddy S M, Park J J, Na S M, et al. *Adv. Funct. Mater.*, **2011**,**21**:4677-4683
(d)Liu M, Lagdani J, Imrane H, et al. *Appl. Phys. Lett.*, **2007**,**90**:103105

[7] Martinho P N, Lemma T, Gildea B, et al. *Angew. Chem. Int. Ed.*, **2012**,**51**:11995-11999

[8] (a)Soyer H, Mingotaud C, Boillot M L, et al. *Langmuir*, **1998**,**14**:5890-5895
(b)Soyer H, Dupart E, Gómez-García C J, et al. *Adv. Mater.*, **1999**,**11**:382-384
(c)Létard J F, Nguyen O, Soyer H, et al. *Inorg. Chem.*, **1999**,**38**:3020-3021
(d)Roubeau O, Agricole B, Clérac, et al. *J. Phys. Chem. B*, **2004**,**108**:15110-15116
(e)Roubeau O, Natividad E, Agricole B, et al. *Langmuir*, **2007**,**23**:3110-3117
(f)White N G, Feltham H L C, Gandolfi C, et al. *Dalton Trans.*, **2010**,**39**:3751-3758
(g)Kitchen J A, White N G, Gandolfi C, et al. *Chem. Commun.*, **2010**,**46**:6464-6466

[9] (a)Ruben M, Rojo J, Romero-Salguero F J, et al. *Angew. Chem. Int. Ed.*, **2004**,**43**:3644-3662
(b)Cobo S, Molnár G, Real J A, et al. *Angew. Chem. Int. Ed.*, **2006**,**45**:5786-5789

[10](a)Jenekhe S A. *Polym. Eng. Sci.*, **1983**,**23**:830-834
(b)Matsuda M, Tajima H. *Chem. Lett.*, **2007**,**36**:700-701
(c)Matsuda M, Isozaki H, Tajima H. *Thin Solid Films*, **2008**,**517**:1465-1467
(d)Quintero C M, Salmon L, Molnár G, et al. *J. Mater. Chem.*, **2012**,**22**:3745-3751
(e)Félix G, Abdul-Kader K, Mahfoud T, et al. *J. Am. Chem. Soc.*, **2011**,**133**:15342-15345
(f)Tissot A, Bardeau J F, Rivière E, et al. *Dalton Trans.*, **2010**,**39**:7806-7812

[11](a)Deegan R D, Bakajin O, Dupont T F, et al. *Nature*, **1997**,**389**:827-829
(b)Galyametdinov Y, Ksenofontov V, Prosvirin A, et al. *Angew. Chem. Int. Ed.*, **2001**,**40**:4269-4271

[12](a)Agusti G, Cobo S, Gaspar A B, et al. *Chem. Mater.*, **2008**,**20**:6721-6732
(b)Bartual-Murgui C, Salmon L, Akou A, et al. *New J. Chem.*, **2011**,**35**:2089-2094

[13](a)Witte G, Wll C. *J. Mater. Res.*, **2004**,**19**:1889-1916
(b)Naggert H, Bannwarth A, Chemnitz S, et al. *Dalton Trans.*, **2011**,**40**:6364-6366
(c)Shi S, Schmerber G, Arabski J, et al. *Appl. Phys. Lett.*, **2009**,**95**:043303

[14](a)Lai P, Hu M Z, Shi D, et al. *Chem. Commun.*, **2008**:1338-1340
(b)Wang Y, Qin Y, Berger A, et al. *Adv. Mater.*, **2009**,**21**:2763-2766
(c)Wang K, Jin S M, Xu J, et al. *ACS Nano*, **2016**,**10**:4954-4960

[15](a)Terekhov S N, Kachan S M, Panarin A Y, et al. *Phys. Chem. Chem. Phys.*, **2015**,**17**:31780-31789
(b)Fang Z, Wang Y, Peng X, et al. *Mater. Lett.*, **2003**,**57**:4187-4190
(c)Cui M, Wang F, Miao Z, et al. *RSC Adv.*, **2015**,**5**:65627-65634

[16](a)Roubeau O. *Chem. Eur. J.*, **2012**,**18**:15230-15244
(b)Sugiyarto K H, Goodwin H A. *Aust. J. Chem.*, **1994**,**47**:263-277

[17](a)Krober J, Codjovi E, Kahn O, et al. *J. Am. Chem. Soc.*, **1993**,**115**:9810-9811
(b)Smit E, Manoun B, Waal D. *J. Raman Spectrosc.*, **2001**,**32**:339-344
(c)Varnek V A, Lavrenova L G. *J. Struct. Chem.*, **1995**,**36**:104-111
(d)Chen Y, Ma J G, Zhang J J, et al. *Chem. Commun.*, **2010**,**46**:5073-5075
(e)Kahn O, Sommier L, Codjovi E. *Chem. Mater.*, **1997**,**9**:3199-3205

[18]He M, Yao J, Low Z X, et al. *RSC Adv.*, **2014**,**4**:7634-7639

[19]Durand P, Pillet S, Bendeif E E, et al. *J. Mater. Chem. C*, **2013**,**1**:1933-1942

[20](a)Hetmańczyk J, Hetmańczyk Ł, Migda-Mikuli A, et al. *J. Raman Spectrosc.*, **2012**,**43**:1118-1125

(b)Abdollahi-Alibeik M, Sadeghi-Vasafi N, Moaddeli A, et al. *Res. Chem. Intermed.*, **2016**,**42**:2867-2881

[21](a)Urakawa A, Van Beek W, Monrabal-Capilla M, et al. *J. Phys. Chem. C*, **2010**,**115**:1323-1329

(b)Grosjean A, Négrier P, Bordet P, et al. *Eur. J. Inorg. Chem.*, **2013**,**2013**:796-802

[22]Chen Y, Ma J G, Zhang J J, et al. *Chem. Commun.*, **2010**, **46**:5073-5075

[23]Lefter C, Tricard S, Peng H, et al. *J. Phys. Chem. C*, **2015, 119**:8522-8529

[24](a)Qiu D, Gu L, Sun X L, et al. *RSC Adv.*, **2014**,**4**:61313-61319

(b)Moussa N O, Ostrovskii D, Garcia V M, et al. *Chem. Phys. Lett.*, **2009**,**477**:156-159

[25](a)Rotaru A, Molnár G, Salmon L, et al. *Chem. Commun.*, **2012**,**48**:4163-4165

(b)Larionova J, Salmon L, Guari Y, et al. *Angew. Chem. Int. Ed.*, **2008**,**120**:8360-8364

(c)Gütlich P, Hauser A, Spiering H. *Angew. Chem. Int. Ed.*, **1994**,**33**:2024-2054

[26]Wang Y X, Qiu D, Xi S F, et al. *Chem. Commun.*, **2016**,**52**: 8034-8037